

NIR J-Aggregates of Hydroazaheptacene Tetraimides

Kang Cai, Jiajun Xie, and Dahui Zhao*

Beijing National Laboratory for Molecular Sciences, Department of Applied Chemistry and the Key Laboratory of Polymer Chemistry and Physics of the Ministry of Education, College of Chemistry, Peking University, Beijing, China

S Supporting Information

ABSTRACT: Hydroazaacene dicarboximide derivatives with red to NIR absorptions are designed and synthesized, which exhibit well-defined J-aggregation behaviors in both solution and thin films. The absorption and emission of an aggregate extend well into the NIR regime ($\lambda_{\text{max}} = 902$ nm), manifesting particularly narrow bandwidth (fwhm = 152 cm^{-1}) and is nearly transparent in the visible region.

Organic molecules with eminent near-infrared (NIR) absorptions attract great interests due to their wide applications in optical and electronic areas.^{1,2} NIR-emitting molecules are even more appealing. Their applications include night vision, optical communication, bioimaging, sensing, etc.^{3,4} NIR active molecules with minimal UV–vis absorptions are useful for transparent photovoltaics, heat-blocking coating, optical filter, information-security display, and so on.⁵

To achieve narrow bandgap in organic molecules, common strategies are to construct large π -conjugate scaffolds and install electron-donating (D) and -accepting (A) groups.^{1,6} NIR-emitting molecules are more difficult to attain, because the energy-gap law intrinsically disfavors the emission of narrow-bandgap systems. Moreover, molecules of large π -systems with D–A features inevitably tend to aggregate strongly. Aggregation-induced quenching further impairs the emission. Thus, designing efficient NIR emitters in the condensed state are particularly challenging.^{7,8}

Here we introduce a series of molecules designed to manifest NIR optical activities by assuming J-aggregation. J-aggregated dyes are of great theoretical interests and practical values.^{9,10} Unique properties of J-aggregates include red-shifted absorptions, narrowed spectral bandwidth, small Stokes shift, and superradiance ability.^{11,12} In terms of structure, J-aggregation requires molecules to stack in a largely slipped arrangement. However, such a packing motif is usually not favored by large conjugated frameworks, because aromatic interactions tend to maximize the face-to-face stacking (i.e., H-aggregate).¹³ As a result, J-aggregated dyes are not abundant and mainly limited to cyanine, squaraines, and chlorophylls.^{12,14} An elegant example of designed J-aggregates was given by Würthner et al. with peryleneimide, by deploying specific hydrogen bonding interactions.¹⁵

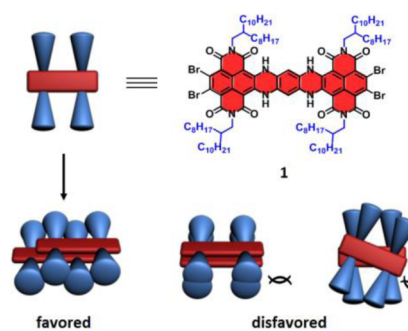
We speculate that the pronounced red shift in the absorption and strong emissions of J-aggregates may be exploited to develop NIR chromophores and emitters. Namely, NIR J-aggregates may be realized with molecules which absorb and emit in the visible region in the single-molecule state. Based on this scheme, NIR J-aggregates are obtained in this study. The most notable aggregate

exhibits intense absorption at 902 nm, with a particularly narrow bandwidth (fwhm = 152 cm^{-1}) at room temperature. Such a wavelength represents one of the lowest J-band energies so far known.¹⁶

After decades of study, there still remain a handful of unsettled issues about the structure and photophysics of J-aggregates.^{11,17} The current molecules, having distinct chemical structures from widely studied J-aggregate dyes but manifesting most well-defined J-aggregation behaviors, may offer new opportunities to unravel certain queries about J-aggregates.

To form J-aggregates, molecules necessarily assume an offset aggregation motif, conducive for coherent exciton coupling (Chart 1). We expect to achieve such molecular packing by

Chart 1. Schematic Representation of Proposed Packing Motifs of Studied Hydroazaheptacene Tetraimide



carefully employing steric interactions.^{15,18} Hydroazaacene tetraimide derivative **1** is specifically designed to form NIR J-aggregates for possessing the following features. First, the molecule has an electron-rich hydroazaheptacene backbone attached with four electron-withdrawing dicarboximide substituents. Our previous study¹⁹ showed that such a unique combination could give rise to narrow bandgap. Second, four branched alkyl groups are tethered to the shape-persistent, band-like polycyclic skeleton. We believe that the number and positions of these side chains are important for J-aggregate formation.²⁰ The exact face-to-face arrangement should be disfavored due to the steric hindrance among the bulky side chains (Chart 1).²¹ Another possibility, the twisted packing motif,^{13b} is also unfavorable due to the repulsive interactions between alkyl side chains and aromatic backbone. Hence, the offset geometry likely becomes the most favorable choice for

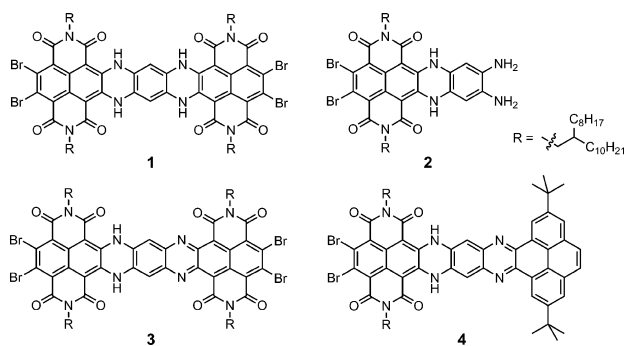
Received: October 7, 2013

Published: December 16, 2013

maintaining substantial aromatic interactions while minimizing the steric hindrance.

The synthesis of molecule **1** started from 2,3,6,7-tetrabromo-1,4,5,10-tetracarboxydiimide (4Br-NDI). At 35 °C, a 1:1 condensation product (**2**) was yielded even if excess benzene-1,2,4,5-tetraamine was added (Chart 2). When the reaction temperature was elevated to 80 °C, further condensation between **2** and 4Br-NDI occurred, affording **1** as a deep green solid (Scheme S1).

Chart 2. Structures of Studied Molecules



The optical properties of **1** in the single-molecule state were first examined. In CHCl_3 solution, compound **1** displayed absorptions in red and NIR regions with clearly resolved vibronic structures. The major peak at 796 nm was assigned to 0–0 transition ($S_0 \rightarrow S_1$, Figure 1a). The energy difference between 0–

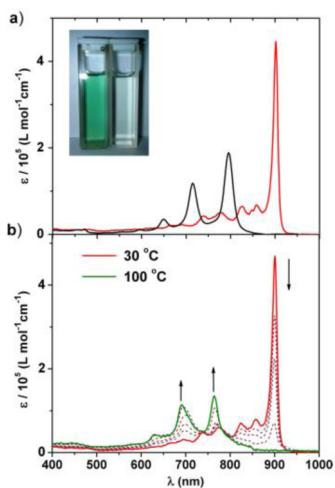


Figure 1. (a) Absorption spectra of **1** (1.0×10^{-6} M) in CHCl_3 (black) and *n*-hexane (red) at room temperature; image shows solutions in CHCl_3 (left) and *n*-hexane (right); (b) absorptions of **1** in *n*-octane (1.0×10^{-6} M) at varied temperatures (arrows indicate the direction of intensity change at increased temperature).

0, 0–1, and 0–2 transitions was consistent with the stretching frequency of aromatic rings.¹¹ The emission spectrum of **1** in the same solvent was a nearly mirror image of its absorption (Figure 2, inset). With the emission maximum at ~ 800 nm, a small Stokes shift of merely 5 nm (79 cm^{-1}) was manifested, evidencing the rigidity of fluorophore skeleton. The fluorescence quantum yield (Φ) of **1** in CHCl_3 was about 8%, which was impressive considering the long wavelengths of emission.

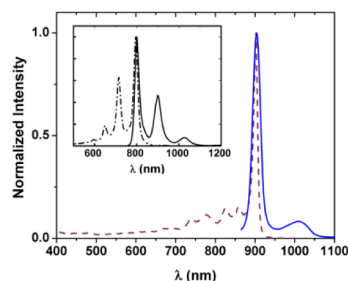


Figure 2. Normalized emission (solid) and absorption (dash) spectra of **1** (1.0×10^{-6} M) in *n*-hexane (excited at 775 nm) and CHCl_3 (inset, excited at 720 nm) at room temperature.

Electrochemical characterizations confirmed that molecule **1** had a rather narrow band gap (Table 1 and Figure S10).

Remarkably, when **1** was dissolved in apolar solvent of *n*-hexane or *n*-octane, a very sharp and much red-shifted absorption peak with large ϵ was detected around 900 nm (Figure 1a). The fwhm of the major peak was reduced from 378 cm^{-1} in CHCl_3 to merely 152 cm^{-1} in *n*-hexane, which was characteristic of coherently delocalized excitonic state.²² Such distinct absorption changes unambiguously indicated that **1** formed J-aggregate in aliphatic solvents. Based on the spectral features, it was estimated that the size of coherent domain in the aggregate was ~ 6 – 7 monomers at room temperature,²³ and the transition dipole moment was approximately enhanced from 13.3 D in monomer to 14.5 D in aggregate.^{15d,22a} Notably, the absorption of the aggregate was shifted well into the NIR regime, with minimal activity in the visible region. Thus, the *n*-hexane solution was nearly colorless, while the CHCl_3 solution had a green color. This J-aggregate was found particularly stable, as no obvious indication of dissociation was shown by the absorption spectrum when the *n*-hexane solution was diluted even to 2×10^{-7} M at room temperature. Upon elevating the temperature of an *n*-octane solution, the absorption peak at 902 nm was observed to attenuate. The molecules were fully dissociated at about 100 °C, as evidenced by the dominance of monomer absorption (Figure 1b). The 0–0 peak of monomer was found at 764 nm at this temperature, corresponding to an energy difference of $\sim 2000 \text{ cm}^{-1}$ between monomer and J-aggregate in *n*-octane. J-aggregated **1** displayed a sharp emission peak at 904 nm in aliphatic solvents, with an fwhm value of $\sim 290 \text{ cm}^{-1}$ (Figure 2). Stokes shift of the aggregate was merely 2 nm ($\sim 25 \text{ cm}^{-1}$). Such significantly red-shifted and nearly vanished Stokes shift further substantiated the J-type identity of the aggregate. It is noteworthy that the aggregate was still emissive and the apparent Φ in *n*-hexane was about 2% (Table 1).

The polycyclic tetraimide skeleton of **1** was a planar structure in the DFT-optimized geometry (Figure S11). Importantly, TD-DFT calculations revealed that the transition dipole moment was oriented along the long axis of hydroazaacene moiety (Figure S12). Hence in the expected sliding packing geometry, the transition dipole of monomers would be favorably oriented, facilitating coherent exciton coupling and emergence of J-aggregate.¹¹

The spectral behaviors of **1** well demonstrated our design of a NIR J-aggregate. In order to further test the hypothesis that the molecular shape is important for promoting J-aggregate, two additional molecules of similar shapes were also synthesized and studied. Molecule **3** was the oxidation product from **1** (Scheme S1), which has nearly identical structure to that of **1** except for losing two hydrogen atoms. Although this molecule has two

Table 1. Optical and Electronic Properties

	λ_{abs}^a [nm]	ϵ^b [L·mol ⁻¹ ·cm ⁻¹]	λ_{em}^c [nm]	Φ^c	λ_{abs}^d (J) ^d [nm]	$\epsilon(J)^e$ [L·mol ⁻¹ ·cm ⁻¹]	λ_{em}^f (J) ^f [nm]	$\Phi(J)^f$	LUMO [eV] ^g	HOMO [eV]	E_g [eV] ^h	LUMO [eV] ^h	HOMO [eV] ^h	E_g^m [eV]
1	796	1.9×10^5	801	0.08	902	4.5×10^5	904	0.02	-3.77	-5.10 ^h	1.33 ^j	-3.39	-5.27	1.88
3	740	9.7×10^4	793	0.05	847	1.4×10^5	869	<0.001	-4.44	-5.82 ^l	1.38 ^k	-4.25	-5.69	1.44
4	651	1.4×10^5	658	0.32	719	2.8×10^5	720	<0.01	-3.31	-4.70 ^h	1.39 ^j	-3.23	-5.30	2.07

^aMonomer absorption maximum in CHCl₃. ^bMolar extinction coefficient at λ_{abs} in CHCl₃. ^cEmission maximum and quantum yield of monomers in CHCl₃. ^dAbsorption maximum of J-band in *n*-hexane. ^eMolar extinction coefficient at $\lambda_{\text{abs}}(J)$ in *n*-hexane. ^fEmission maximum and apparent quantum yield in *n*-hexane. ^gLUMO from CV. ^hHOMO from CV. ⁱHOMO based on optical band gap from absorption spectrum and CV-determined LUMO. ^jBand gap from CV-determined LUMO and HOMO. ^kOptical band gap based on the monomer absorption onset in CHCl₃. ^mDFT calculated results.

possible tautomers (benzenoid and quinonoid), only benzenoid tautomer **3** was detected, which was confirmed with NMR spectra by drawing analogy with previously reported molecules of closely related structure.¹⁹

The absorption of **3** in the single-molecule state displayed a major peak at 740 nm in CHCl₃ (Figure 3). TD-DFT

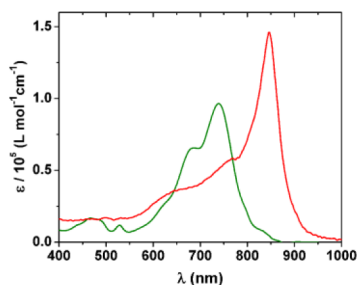


Figure 3. Absorption spectra of **3** in CHCl₃ (green) and *n*-hexane (red) at room temperature (1.5×10^{-6} M).

calculations showed that this band mainly originated from a mixed transition from HOMO-2 and HOMO-3 to LUMO (Figure S11), which explained its relatively broad bandwidth. In *n*-hexane, the absorption was red-shifted to nearly 850 nm, while the bandwidth was evidently narrowed (Figure 3). Both these features indicated the J-aggregate formation. Monomer **3** had a lower emission Φ than **1**, and the emission of aggregated **3** was vastly quenched. Based on the trace emission from *n*-hexane solution, the fluorescence of aggregate was shifted to 868 nm, compared to 790 nm of monomer in CHCl₃ (Figures S5 and S6). Smaller Stokes shift and narrowed emission bandwidth were also observed for aggregate **3**.

Compound **4**, prepared via condensation between **2** and 2,7-di(*tert*-butyl)pyrene-4,5-dione (Scheme S1), also had a dihydrotetraazaheptacene moiety, but one of the NDI subunits was replaced by a pyrene group. Two *t*-butyl groups were installed on pyrene to confer similar steric effect as in **1** and **3**. While monomer **4** showed multiple absorption vibration peaks in CHCl₃, the 0–0 transition at 650 nm was shifted to 718 nm in *n*-hexane (Figure 4a). A much narrower bandwidth (fwhm = 332 cm⁻¹ in *n*-hexane vs 544 cm⁻¹ in CHCl₃) was also displayed, corresponding to a coherent length of roughly 2–3 monomers in the J-aggregate.²³ The transition dipole moment was calculated to increase from about 9.38 D for monomer to ~9.94 D in the aggregate. The association strength of **4** appeared weaker than that of **1**. Its reversible association–dissociation process could be followed by collecting absorption spectra at varied concentrations (Figure 4b). Diminished J-band at lower concentrations proved its origin from intermolecular aggregation. With the monomer absorption maximum shown at 636 nm, an energy

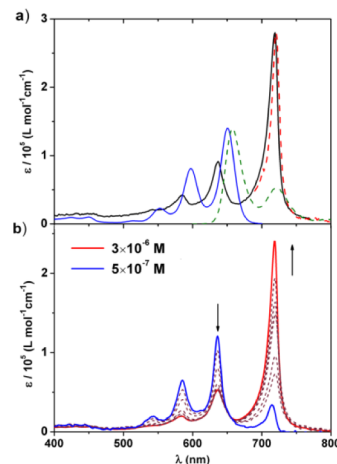


Figure 4. (a) Absorption (solid) and emission (dash) spectra of **4** (1.0×10^{-6} M) in CHCl₃ (blue and green) and *n*-hexane (black and red); (b) varied-concentration absorptions of **4** in *n*-hexane (arrows indicate the direction of change at increased concentrations).

shift of 1795 cm⁻¹ from monomer to J-aggregate was identified for **4**. The temperature dependence of absorption revealed that the dissociation of aggregate **4** was completed at about 60 °C at 2.0×10^{-6} M in *n*-octane (Figure S7).

Although monomer **4** was fairly emissive in CHCl₃ ($\Phi = 0.32$), the emission of aggregate **4** was mostly quenched. The major emission peak of aggregated **4** nearly superimposed with its J-band, showing a Stokes shift of merely 25 cm⁻¹ or so (Figure 4a). In addition to this peak at 720 nm, another emission peak was detected at ~850 nm (Figure S7), which likely originated from excimer species.

Thin films of **1**, **3**, and **4** were prepared by drop-casting respective solutions in *n*-hexane (1.0×10^{-4} M) on quartz slides. Very similar absorption and emission features were displayed by thin films to those in aliphatic solvents (Figure S9), indicating similar aggregated structures under both conditions. Molecules **1** and **4** were still emissive in thin films, while the emission of **3** was completely quenched.

In summary, three novel hydroazaacene dicarboximide derivatives were synthesized, all of which exhibited significantly red-shifted absorptions with narrowed band widths and smaller Stokes shifts in aliphatic solvents, evidencing J-aggregate formation. Aggregated **1** and **3** absorbed strongly in the NIR range, with maxima near 900 and 850 nm, respectively. With an absorption fwhm of only 152 cm⁻¹, J-aggregated **1** was nearly transparent to the visible light and emitting NIR light. Such properties made it useful NIR materials.

The fact that three molecules having different backbones but similar shapes all formed J-aggregates well illustrated the

hypothesis that the molecule geometry was relevant to the J-aggregate formation in this system. With polycyclic backbones providing the driving force for molecular stacking, carefully designed steric interactions facilitated the slipped packing motif. As a new type of structure exhibiting typical J-aggregate features, these molecules will be of values for better understanding the J-aggregates through further studies.

■ ASSOCIATED CONTENT

■ Supporting Information

Experimental procedures and analytical data. This material is available free of charge via the Internet at <http://pubs.acs.org>.

■ AUTHOR INFORMATION

Corresponding Author

dhzhao@pku.edu.cn

Notes

The authors declare no competing financial interest.

■ ACKNOWLEDGMENTS

We acknowledge the financial support of the National Natural Science Foundation of China (Projects 21174004, 21222403 and 51073002).

■ REFERENCES

- (1) (a) Fabian, J.; Nakanzumi, H.; Matsuoka, M. *Chem. Rev.* **1992**, *92*, 1197. (b) Weil, T.; Vosch, T.; Hofkens, J.; Peneva, K.; Müllen, K. *Angew. Chem., Int. Ed.* **2010**, *49*, 9068. (c) Gang, Q.; Wang, Z. *Chem. Asian J.* **2010**, *5*, 1006.
- (2) (a) Mayerhöffer, U.; Deing, K.; Gruf, K.; Braunschweig, H.; Müllen, K.; Würthner, F. *Angew. Chem., Int. Ed.* **2009**, *48*, 8776. (b) Imahori, H.; Umeyama, T.; Ito, S. *Acc. Chem. Res.* **2009**, *42*, 1809. (c) Bürckstümmer, H.; Kronenberg, N. M.; Meerholz, K.; Würthner, F. *Org. Lett.* **2010**, *12*, 3666. (d) Qian, G.; Qi, J.; Davey, J. A.; Wright, J. S.; Wang, Z. Y. *Chem. Mater.* **2012**, *24*, 2364.
- (3) (a) Ghorroghchian, P. P.; Frail, P. R.; Susumu, K.; Blessington, D.; Brannan, A.; Bates, F. S.; Chance, B.; Hammer, D. A.; Therien, M. J. *Proc. Natl. Acad. Sci. U.S.A.* **2005**, *102*, 2922. (b) Koide, Y.; Urano, Y.; Hanaoka, K.; Piao, W.; Kusakabe, M.; Saito, N.; Terai, T.; Okabe, T.; Nagano, T. *J. Am. Chem. Soc.* **2012**, *134*, 5029. (c) Yuan, L.; Lin, W.; Yang, Y.; Chen, H. *J. Am. Chem. Soc.* **2012**, *134*, 1200.
- (4) (a) Borek, C.; Hanson, K.; Djurovich, P. I.; Thompson, M. E.; Aznavour, K.; Bau, R.; Sun, Y.; Forrest, S. R.; Brooks, J.; Michalski, L.; Brown, J. *Angew. Chem., Int. Ed.* **2007**, *119*, 1127. (b) Qian, G.; Zhong, Z.; Luo, M.; Yu, D.; Zhang, Z.; Wang, Z. Y.; Ma, D. *Adv. Mater.* **2009**, *21*, 111. (c) Graham, K. R.; Yang, Y.; Sommer, J. R.; Shelton, A. H.; Schanze, K. S. *Chem. Mater.* **2011**, *23*, 5305. (d) Yuan, L.; Lin, W.; Zhao, S.; Gao, W.; Chen, B.; He, L.; Zhu, S. *J. Am. Chem. Soc.* **2012**, *134*, 13510.
- (5) (a) Bachmann, F. G.; Russek, U. A. *SPIE* **2002**, *4637*, 505. (b) Lunt, R. R.; Bulovic, V. *Appl. Phys. Lett.* **2011**, *98*, 113305. (c) Fischer, G. M.; Daltrozzo, E.; Zumbusch, A. *Angew. Chem., Int. Ed.* **2011**, *50*, 1406. (d) Su, Y.; Zhou, X.; Chen, H.; Tan, J.; Hu, T.; Yan, J.; Peng, P. *Appl. Phys. Lett.* **2012**, *101*, 041913.
- (6) (a) Avlasevich, Y.; Müllen, K. *Chem. Commun.* **2006**, 4440. (b) Fischer, G. M.; Ehlers, A. P.; Zumbusch, A.; Daltrozzo, E. *Angew. Chem., Int. Ed.* **2007**, *46*, 3750. (c) Qian, G.; Dai, B.; Luo, M.; Yu, D.; Zhan, J.; Zhang, Z.; Ma, D.; Wang, Z. Y. *Chem. Mater.* **2008**, *20*, 6208. (d) Luo, M.; Shadnia, H.; Qian, G.; Du, X.; Yu, D.; Ma, D.; Wright, J. S.; Wang, Z. Y. *Chem.—Eur. J.* **2009**, *15*, 8902. (e) Jiao, C.; Huang, K.-W.; Luo, J.; Zhang, K.; Chi, C.; Wu, J. *Org. Lett.* **2009**, *11*, 4508. (f) Mayerhöffer, U.; Fimmel, B.; Würthner, F. *Angew. Chem., Int. Ed.* **2012**, *51*, 164. (g) Karton-Lifshin, N.; Albertazzi, L.; Bendikov, M.; Baran, P. S.; Shabat, D. *J. Am. Chem. Soc.* **2012**, *134*, 20412.
- (7) (a) D'Aléo, A.; Gachet, D.; Heresanu, V.; Giorgi, M.; Fages, F. *Chem.—Eur. J.* **2012**, *18*, 12764. (b) Zhao, Q.; Zhang, S.; Liu, Y.; Mei, J.;

Chen, S.; Lu, P.; Qin, A.; Ma, Y.; Sun, J. Z.; Tang, B. Z. *J. Mater. Chem.* **2012**, *22*, 7387.

(8) Du, X.; Qi, J.; Zhang, Z.; Ma, D.; Wang, Z. Y. *Chem. Mater.* **2012**, *24*, 2178.

(9) (a) Borsenberger, P. M.; Chowdry, A.; Hoesterey, D. C.; Mey, W. J. *Appl. Phys.* **1978**, *44*, 5555. (b) Chatterjee, S.; Davis, P. D.; Gottschalk, P.; Kurz, M. E.; Sauerwein, B.; Yang, X.; Schuster, G. B. *J. Am. Chem. Soc.* **1990**, *112*, 6329. (c) Wang, Y. *J. Opt. Soc. Am. B* **1991**, *8*, 981. (d) Tischler, J. R.; Bradley, M. S.; Bulović, V.; Song, J. H.; Nurmikko, A. *Phys. Rev. Lett.* **2005**, *95*, 036401. (e) Walker, B. J.; Nair, G. P.; Marshall, L. F.; Bulović, V.; Bawendi, M. G. *J. Am. Chem. Soc.* **2009**, *131*, 9624.

(10) (a) Holzwarth, A. R.; Schaffner, K. *Photosynth. Res.* **1994**, *41*, 225. (b) Pullerits, T.; Sundström, V. *Acc. Chem. Res.* **1996**, *29*, 381. (c) Huber, V.; Katterle, M.; Lysetska, M.; Würthner, F. *Angew. Chem., Int. Ed.* **2005**, *44*, 3147.

(11) Spano, F. C. *Acc. Chem. Res.* **2009**, *43*, 429.

(12) (a) *J-Aggregates*; Kobayashi, T., Ed.; World Scientific: Singapore, 1996; (b) *J-Aggregates (volume 2)*; Kobayashi, T., Ed.; World Scientific: Singapore, 2012; (c) Möbius, D. *Adv. Mater.* **1995**, *7*, 437. (d) Würthner, F.; Kaiser, T. E.; Möller, C. R. S. *Angew. Chem., Int. Ed.* **2011**, *50*, 3376.

(13) (a) Würthner, F. *Chem. Commun.* **2004**, *14*, 1564. (b) Chen, Z.; Lohr, A.; Saha-Möller, C. R.; Würthner, F. *Chem. Soc. Rev.* **2009**, *38*, 564. (c) Rösch, U.; Yao, S.; Wortmann, R.; Würthner, F. *Angew. Chem., Int. Ed.* **2006**, *45*, 7026.

(14) (a) Barber, D. C.; Beeston, R. A. F.; Whitten, D. G. J. *Phys. Chem.* **1991**, *95*, 4074. (b) Castriciano, M. A.; Romeo, A.; Villari, V.; Micali, N.; Scolaro, L. M. *J. Phys. Chem. B* **2003**, *107*, 8765. (c) Kameyama, K.; Morisue, M.; Satake, A.; Kobuke, Y. *Angew. Chem., Int. Ed.* **2005**, *44*, 4763.

(15) (a) Kaiser, T. E.; Wang, H.; Stepanenko, V.; Würthner, F. *Angew. Chem., Int. Ed.* **2007**, *46*, 5541. (b) Yagai, S.; Seki, T.; Karatsu, T.; Kitamura, A.; Würthner, F. *Angew. Chem., Int. Ed.* **2008**, *47*, 3367. (c) Würthner, F.; Bauer, C.; Stepanenko, V.; Yagai, S. *Adv. Mater.* **2008**, *20*, 1695. (d) Kaiser, T. E.; Stepanenko, V.; Würthner, F. *J. Am. Chem. Soc.* **2009**, *131*, 6719. (e) Xie, Z.; Stepanenko, V.; Radacki, K.; Würthner, F. *Chem.—Eur. J.* **2012**, *18*, 7060.

(16) (a) Pullerits, T.; Sundström, V. *Acc. Chem. Res.* **1996**, *29*, 381. (b) Hannah, K. C.; Armitage, B. A. *Acc. Chem. Res.* **2004**, *37*, 845. (c) Wang, H.; Kaiser, T. E.; Uemura, S.; Würthner, F. *Chem. Commun.* **2008**, 1181.

(17) (a) Eisele, D. M.; Knoester, J.; Kirstein, S.; Rabe, J. P.; Vanden Bout, D. A. *Nat. Nanotechnol.* **2009**, *4*, 658. (b) Lin, H.; Camacho, R.; Tian, Y.; Kaiser, T. E.; Würthner, F.; Scheblykin, I. G. *Nano Lett.* **2010**, *10*, 620. (c) Eisele, D. M.; Cone, C. W.; Bloemsma, E. A.; Vlaming, S. M.; van der Kwaak, C. G. F.; Silbey, R. J.; Bawendi, M. G.; Knoester, J.; Rabe, J. P.; Vanden Bout, D. A. *Nat. Chem.* **2012**, *4*, 655. (d) Pati, A. J.; Lee, Y.-C.; Yan, J.-W.; Mann, S. *Angew. Chem., Int. Ed.* **2012**, *124*, 757.

(18) Chan, J. M.; Tischler, J. R.; Kooi, S. E.; Bulović, V.; Swager, T. M. *J. Am. Chem. Soc.* **2009**, *131*, 5659.

(19) Cai, K.; Yan, Q.; Zhao, D. *Chem. Sci.* **2012**, *3*, 3175.

(20) We also examined a number of other N-heterocyclic dicarboximide derivatives previously published in ref 19, which had similar backbones but only two imide side groups. None of those molecules exhibited well-defined J-aggregate features.

(21) (a) Chen, Z.; Stepanenko, V.; Dehm, V.; Prins, P.; Siebbeles, L. D. A.; Seibt, J.; Marquetand, P.; Engel, V.; Würthner, F. *Chem.—Eur. J.* **2007**, *13*, 436. (b) Lim, J. M.; Kim, P.; Yoon, M.-C.; Sung, J.; Dehm, V.; Chen, Z. *Chem. Sci.* **2013**, *4*, 388.

(22) (a) Liptay, W.; Wortmann, R.; Schaffrin, H.; Burkhard, O.; Reitingner, W.; Detzer, N. *Chem. Phys.* **1988**, *120*, 429. (b) Knoester, F. *J. Chem. Phys.* **1993**, *99*, 8566.

(23) The size of coherent domain (N) was calculated from: $\text{fmwh}_{\text{mon}}/\text{fmwh}_{\text{agg}} = \sqrt{N}$. This equation assumes that fwhm of J-band is solely determined by motional narrowing, but the actual coherent size should be larger when other mechanisms of line broadening (e.g., temperature or disorder) occur. See refs: (a) Knapp, E. W. *Chem. Phys.* **1984**, *1*, 73. (b) Koti, A. S. R.; Taneja, J.; Periasamy, N. *Chem. Phys. Lett.* **2003**, *375*, 171. (c) Busse, G.; Frederichs, B.; Petrov, N. K.; Techert, S. *Phys. Chem. Chem. Phys.* **2004**, *6*, 3309.